

Aggregation of Antifreeze Glycoprotein Fraction 8 and Its Effect on Antifreeze Activity

Vincent R. Bouvet, Gianni R. Lorello, and Robert N. Ben*

Department of Chemistry, 10 Marie Curie, University of Ottawa, Ottawa, Ontario, Canada K1N 6N5

Received August 22, 2005; Revised Manuscript Received November 17, 2005

Antifreeze glycoproteins (AFGPs) have many potential applications ranging from the cryopreservation and hypothermic storage of tissues and organs to the preservation of various frozen food products. Since supplying native AFGP for these applications is a labor-intensive and costly process, the rational design and synthesis of functional AFGP analogues is a very attractive alternative. While structure–function studies have implicated specific structural motifs as essential for antifreeze activity in AFGP, the relationship between solution conformation and antifreeze activity is poorly understood. Toward this end, we have analyzed AFGP8 in aqueous solutions using dynamic light scattering (DLS) and circular dichroism (CD). Our results indicate that AFGP8 forms discrete aggregates in solution. These aggregates are predominantly composed of dimers that form at solution concentrations greater than 20 mM. CD spectroscopy indicates that the preferred solution conformation of AFGP8 is consistent with that of random coil. However, significant β -sheet and α -helix character is observed in more concentrated solutions, indicating that these glycopeptides are highly flexible in solution. Aggregation appears to have a minimal effect on the overall solution conformation. Thermal hysteresis (TH) activity of the aggregated solutions is much higher than that of less concentrated solutions that do not form aggregates. While cooperative functioning between lower and higher molecular weight AFGPs has been reported, this is the first instance where cooperative functioning in lower molecular weight AFGPs has been observed.

Introduction

Antifreeze glycoproteins (AFGPs) are found in many deep-sea teleost fish.^{1,2} While the physiological concentration of these glycoproteins varies throughout the year, they efficiently protect these organisms against cryoinjury and death. AFGPs are glycopolymers possessing a repeating Thr-Ala-Ala tripeptide unit and the secondary hydroxyl group is glycosylated with a β -D-galactosyl-(1,3)- α -N-acetyl-D-galactosaminyl disaccharide (Figure 1). These glycopolymers have been divided into eight classes based upon molecular mass such that AFGP8 ($n = 4$) is 2.6 kDa and AFGP1 is 33 kDa. In some of the lower molecular mass fractions (i.e., AFGP7–8), the threonine residue may be substituted with an arginine residue and one or both alanine residues may be substituted with proline.³

The mechanism of action by which these compounds function is an adsorption-inhibition process where AFGPs bind irreversibly to the surface of an ice crystal and elicit a localized freezing-point depression.⁴ The structural moieties crucial for the AFGP–ice interaction remain a source of debate among experts in the field.^{5–7} Recent structure–function studies have implicated the disaccharide, β -methyl group of threonine, and the C-2 acetamide moieties as essential for potent antifreeze activity.⁸

The relationship between AFGP activity and solution conformation has been previously examined by a number of research groups in a concerted effort to understand how AFGPs elicit a localized freezing-point depression.^{9–12} Toward this end, a number of complementary techniques have been employed and generated somewhat contradictory results. Early circular dichroism (CD) studies suggest AFGPs adopt a random coil conformation in solution,^{10,13–14} while vacuum ultraviolet CD experiments imply a 3-fold left-handed helix¹⁵ (but the data are

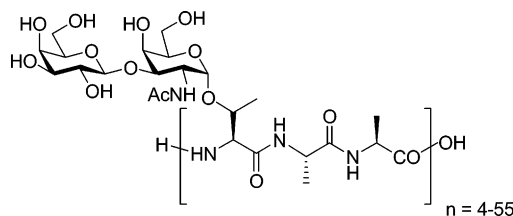


Figure 1. Typical antifreeze glycoprotein (AFGP).

not inconsistent with a random coil structure). Quasi-elastic light scattering (QELS or DLS) studies suggest an extended coil is the predominant conformation,¹⁶ but Raman spectroscopy implies a random coil with significant α -helix and β -conformations.¹⁷ Analysis of the solution conformation of AFGP 1–4 and AFGP8 by ¹H NMR supports the existence of a 3-fold left-handed helix^{11,18} previously observed by vacuum UV circular dichroism. Early ¹³C NMR experiments propose a random coil structure¹⁹ as well as a flexible coil structure.²⁰ In lieu of these conflicting results, a more distinct picture has recently emerged through the use of high-field NMR, IR spectroscopy, and molecular dynamics simulations.^{21,22} These studies suggest that AFGP1–5 is a dynamically disordered molecule showing neither long- nor short-range order. In contrast, AFGP8 appears to possess no long-range order but does possess local order consistent with a polyproline II structure. While these studies suggest that the 3D solution conformation of AFGP is very complicated, the relationship between activity and conformation is still not understood and additional studies are required.

We have previously reported differences in the adsorption of AFGP8 onto both hydrophobic (HOPG) and hydrophilic (mica and silica) surfaces.²³ In these studies AFGP8 (2.6 kDa) was obtained from A/F Protein Inc. and isolated from the cold ocean teleost species *Gadus ogac* (rock cod). The lyophilized glycoprotein was 95% pure (HPLC) with small amounts of

* Corresponding author: e-mail Robert.Ben@science.uottawa.ca.

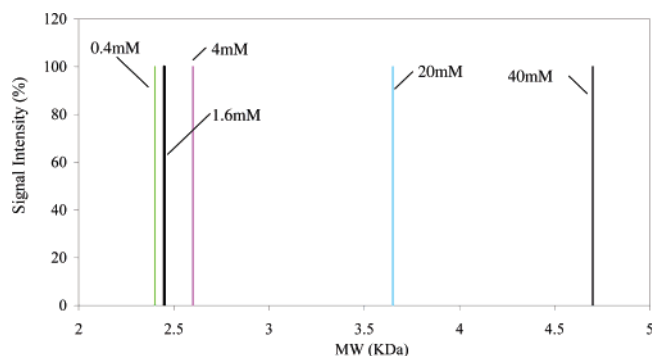


Figure 2. Dynamic light scattering of filtered AFGP8 solutions in distilled water.

AFGP7 and other naturally occurring plasma proteins present.²⁴ Our atomic force microscopy (AFM) studies suggested that, unlike AFGP1–5, AFGP8 forms aggregates in solution prior to adsorption onto both hydrophilic and hydrophobic surfaces. While the issue of glycoprotein aggregation is itself very interesting, the implications of AFGP8 aggregation and its effects on solution conformation and antifreeze activity have not been studied. Since atomic force microscopy is not a suitable technique to explore the aggregation of AFGP, we sought to examine this phenomenon using dynamic light scattering (DLS) and circular dichroism (CD), two techniques that have a time scale between those of IR and NMR.

Results

Dynamic Light Scattering Experiments. Dynamic light scattering experiments were performed on a DynaPro dynamic light scattering apparatus in distilled water at concentrations ranging from 0.4 to 40 mM. The correlation curves were interpreted with the Dynamics Software version 6.1.08. This software is appropriate to fit correlation curves exhibiting multiple exponential decays (i.e., solutions that are multimodal in nature). All the discontinuous correlation curves as well as correlation curves exhibiting outlier sum of squares analysis (SOS) due to aberrant effects (dust, etc.) have been excluded. Solution concentrations greater than 40 mM were not examined due to the high viscosity and the inherent error associated with estimating molecular weights in such solutions. Initial DLS experiments revealed the presence of a high molecular mass substance exceeding 10 000 kDa (data not shown). Despite careful efforts to ensure the samples were dust-free, the high molecular weight substance was attributed to particulates. This was problematic in that a PMT saturation effect was observed when 100% laser power was used. However, by employing a 65% reduction in laser power, the samples could be analyzed. Under these conditions an 8 kDa aggregate that had 1% the signal intensity but corresponded to 99.9% of the sample mass was sporadically observed at higher AFGP8 concentrations. Given that the scattering of light in DLS is exponentially proportional to the size of the aggregate in solution, the detection of these small aggregates in the presence of particles in excess of 10 000 kDa was difficult with reduced laser power. However, filtration with a 100 kDa nanopore filter removed the particulates and permitted a higher laser power to be used. Under these conditions, analysis of the 20 and 40 mM solutions (Figure 2) revealed the presence of aggregates consistent in size with at least two individual AFGP8 molecules.²⁵ Figure 2 describes the average aggregate size for various solutions. Each solution was observed over 20 measurements and shows an overall molecular

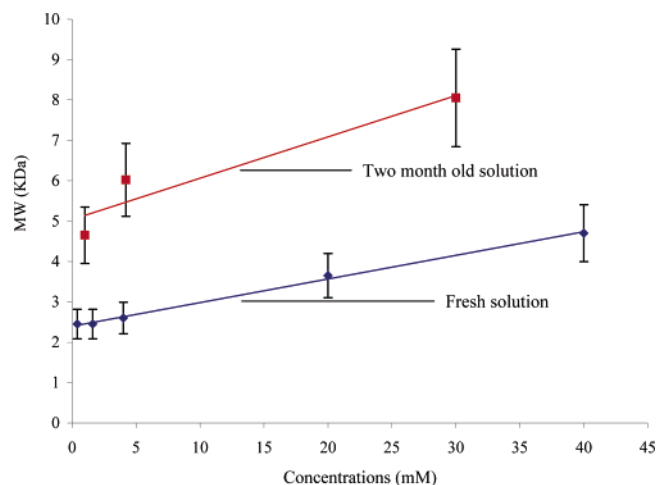


Figure 3. Aggregate size as a function of concentration and time. All solutions were filtered with a 100 kDa Nanopore filter prior to analysis.

mass increase as a function of solution concentration. In contrast, 0.4–4 mM solutions of AFGP8 showed no evidence of aggregation.

We have investigated this aggregation process as a function of time and solution concentration (Figure 3). These experiments confirm the propensity for the aggregates to increase in size when left suspended in solution. For instance, a freshly prepared 1 mM solution of AFGP8 initially showed no evidence of aggregation, but analysis of a similar solution allowed to stand for 2 months revealed aggregates consistent with AFGP8 dimers (molecular mass approximately 5.0 kDa).

It was also observed that the initial concentration of the AFGP8 solution had an influence on the size of aggregate formed. For instance, a freshly prepared 40 mM solution contained aggregates of two AFGP molecules (5.0 kDa) while a 1 mM solution contained only monomers. The low polydispersity and the continuity in the correlation curves associated with a high sum of squares (SOS) value ruled out the presence of dust and suggested we were observing a multimodal system with low polydispersities. Figure 4 depicts the multimodality of the aggregates in 20 and 40 mM solutions of AFGP8. This example is the result of 20 measurements without any molecular weight averaging. Each measurement represents a weighted average of 11 acquisitions; thus, 20 measurements were taken for a total of 220 acquisitions. The error bars in Figure 4 represent the mean standard deviation obtained from each measurement. The 40 mM solution of AFGP8 in water produces aggregates consistent with two individual AFGP8 molecules, while the 20 mM solution contained predominantly individual AFGP8 molecules.

On the basis of the DLS results, we sought to investigate whether the aggregation significantly influenced solution conformation. Toward this end, we examined the solution conformation of AFGP8 as a function of concentration and temperature by circular dichroism (CD) spectroscopy.

Circular Dichroism. All CD measurements were obtained on a Jasco 810 CD spectrometer, and samples were dissolved in double-distilled water without any buffer at pH = 7.4. Deconvolution analysis was performed by use of CDPro with SELCON3 and IBASIS5. This method has been shown to accurately estimate the secondary structure of a large number of proteins with assorted secondary structures.²⁶

At 21 °C, 0.01–0.05 mM solutions of AFGP8 produced spectra consistent with random coil structure (Figure 5).

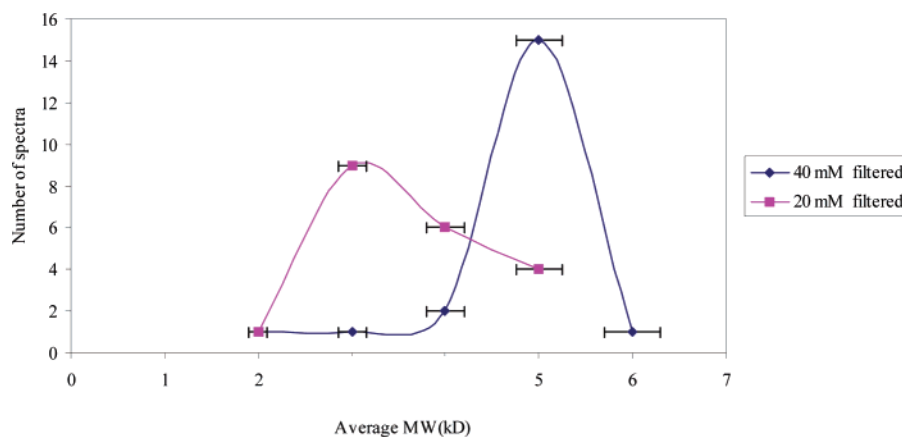


Figure 4. Multimodality of AFGP 8 at different concentrations.

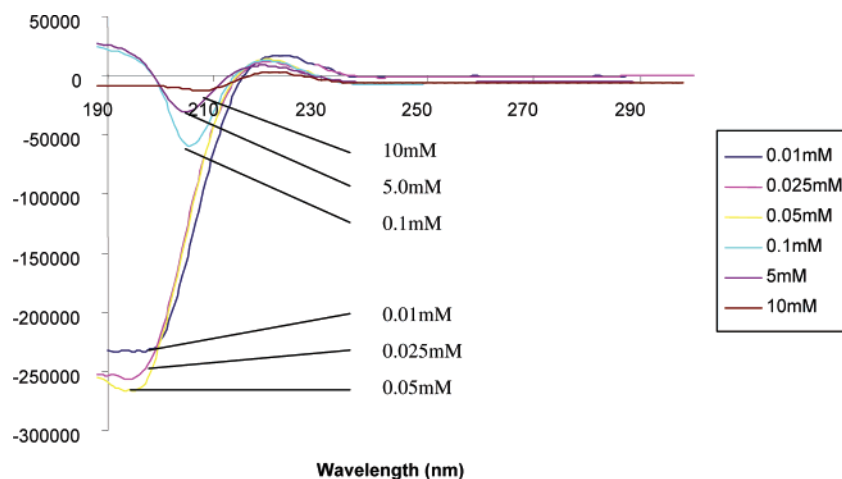


Figure 5. CD spectrum of AFGP8 in distilled H₂O as a function of concentration at 21 °C.

Deconvolution of these spectra indicated that the major conformation present in solution was random coil (41%) with 13% α -helix, 20% β -sheet, and smaller percentages of β -turn and polyproline type II helix.

At concentrations of 0.1 and 5.0 mM, the CD spectrum of AFGP8 changed dramatically and exhibited a large positive Cotton effect at 195 nm. Estimation of the secondary structure with deconvolution software suggested this was the result of a 17% increase in α -helix content in the glycopeptide. The relative amount of random coil structure remained constant at 41%, while the relative contribution for β -sheet conformation was reduced by 8%. A 10 mM solution of AFGP8 was approximately 85% random coil. This dynamic “mixture” of conformations was also reflected in the absence of a well-defined isodichroic point, consistent with a system possessing more than a two-state conformational equilibrium.

At higher concentrations (20–100 mM), other dramatic changes in the CD spectra were evident (Figure 6). Deconvolution of these spectra revealed subtle changes in the local conformational ordering. The relative amount of random coil was between 40% and 48% with contributions from β -sheet structure at 35%. In the 70, 80, 90, and 100 mM AFGP8 solutions, the contribution of random coil secondary structure was approximately equal and β -sheet contributions were still the second most predominant contributor. All of these spectra, including those in Figure 5, reflected a small degree of polyproline II character ranging between 6% and 17%. A slight red shift was also observed with the very concentrated AFGP8 solutions.

Given the possibility that the conformation of AFGP8 might be different at lower temperatures, CD measurements were performed on the same samples at -0.5 °C (Figures 7 and 8). The 0.5 and 1.0 mM solutions of AFGP8 possessed identical percentages of random coil (41%) and β -sheet (20%) secondary structures when compared to the same solutions at room temperature. α -Helix, polyproline II, and β -turn secondary structures were equal contributors (approximately 13% each) to the remaining secondary structure. In contrast, the 5 mM AFGP8 solution possessed random coil as the predominant secondary structure (40%), but an 18% increase in the percentage of α -helix was observed. Interestingly, the ratio of random coil to α -helical content was identical to the 5 mM solution at 21 °C with 30% total α -helix. The 10 mM AFGP8 solution exhibited a secondary structure of random coil (42%) with approximately 34% β -sheet.

At -0.5 °C, the 20–100 mM solutions of AFGP8 exhibited varying degrees of random coil (20–55%) and β -sheet (37–45%) as the predominant secondary structures in solution. While these two conformations accounted for 80–90% of the solution conformations, it is likely that other conformations are present in solution based upon the fact that a well-defined isodichroic point was not observed. As with the CD spectra at 21 °C, a slight red shift was observed with increasing concentration.

Correlating Aggregation as a Function of Antifreeze Activity. The most interesting aspect of AFGP8 aggregation is not that discrete aggregates are formed but rather the effect these aggregates may have on antifreeze activity. The accepted “standard” for assessment of antifreeze activity is thermal

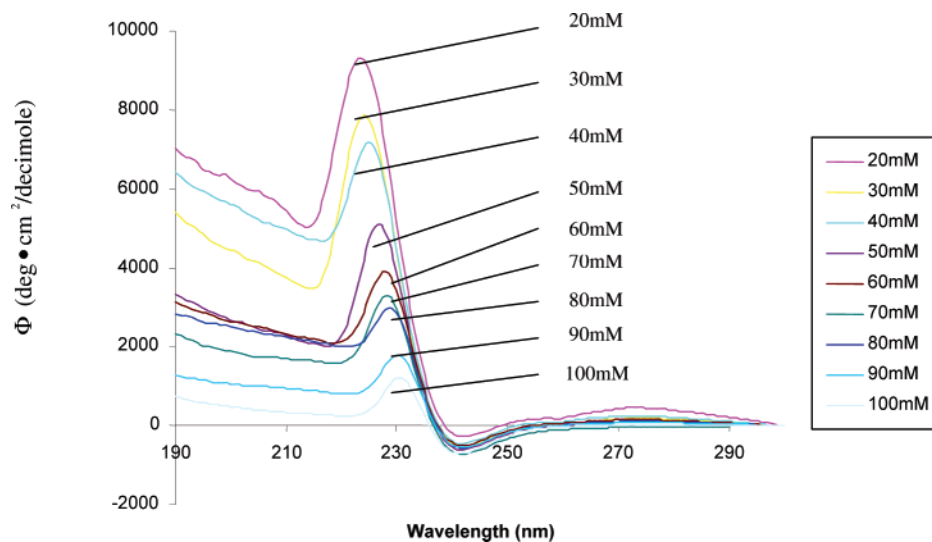


Figure 6. CD spectrum of AFGP8 in distilled H₂O as a function of concentration at 21 °C.

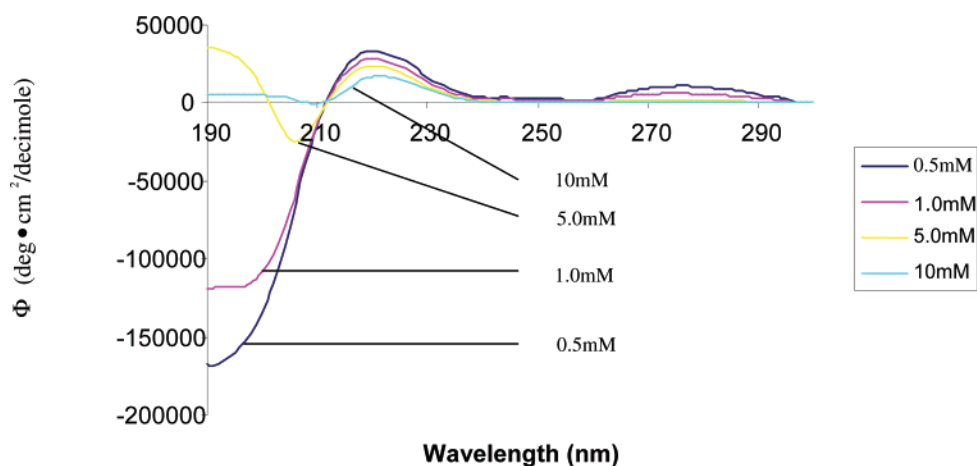


Figure 7. CD spectrum of AFGP8 in distilled H₂O as a function of concentration (0.5–10 mM) at -0.5 °C.

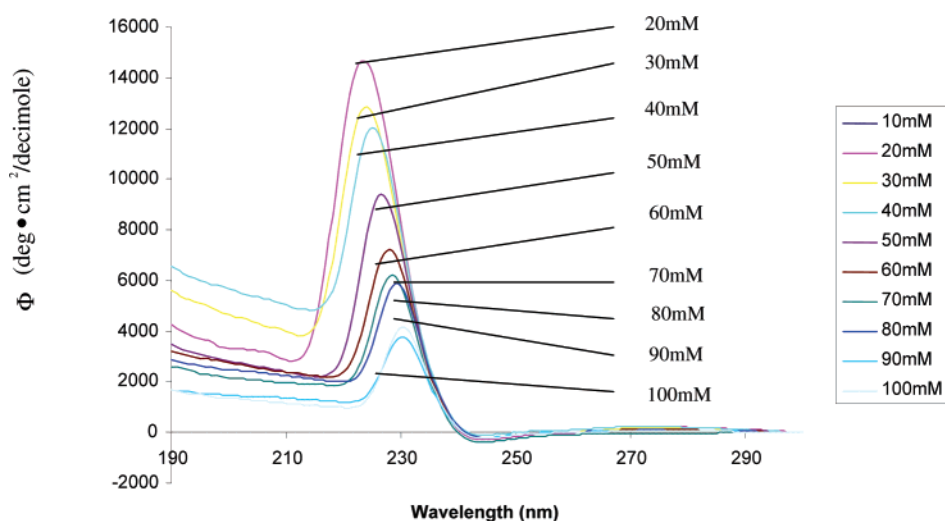


Figure 8. CD spectrum of AFGP8 in distilled H₂O as a function of concentration (10–100 mM) at -0.5 °C.

hysteresis by use of a Nanoliter Osmometer (Clifton Technical Physics).^{27,28} The TH profile for AFGP8 isolated from *Gadus ogac* has been reported for concentrations ranging from 1 to 20 mg/mL (0.4–7.5 mM).²⁴ In contrast, we have assessed TH activity over a much wider concentration range (0.05–60 mM) (Figure 9). All measurements were performed three times and the freezing point was recorded once “burst crystal growth” occurred. While our TH values are slightly higher than those

previously reported, this was attributed to a small amount of AFGP7 present in the sample. Solutions of AFGP8 up to 10 mM exhibit a TH profile typical of a noncolligatively acting biological antifreeze. The plateau observed between 10 and 35 mM is also consistent with a noncolligative effect. However, the TH profile increased sharply above 35 mM and continued to increase in a linear fashion, indicating that AFGP8 solutions ranging in concentration from 40 to 60 mM are much more

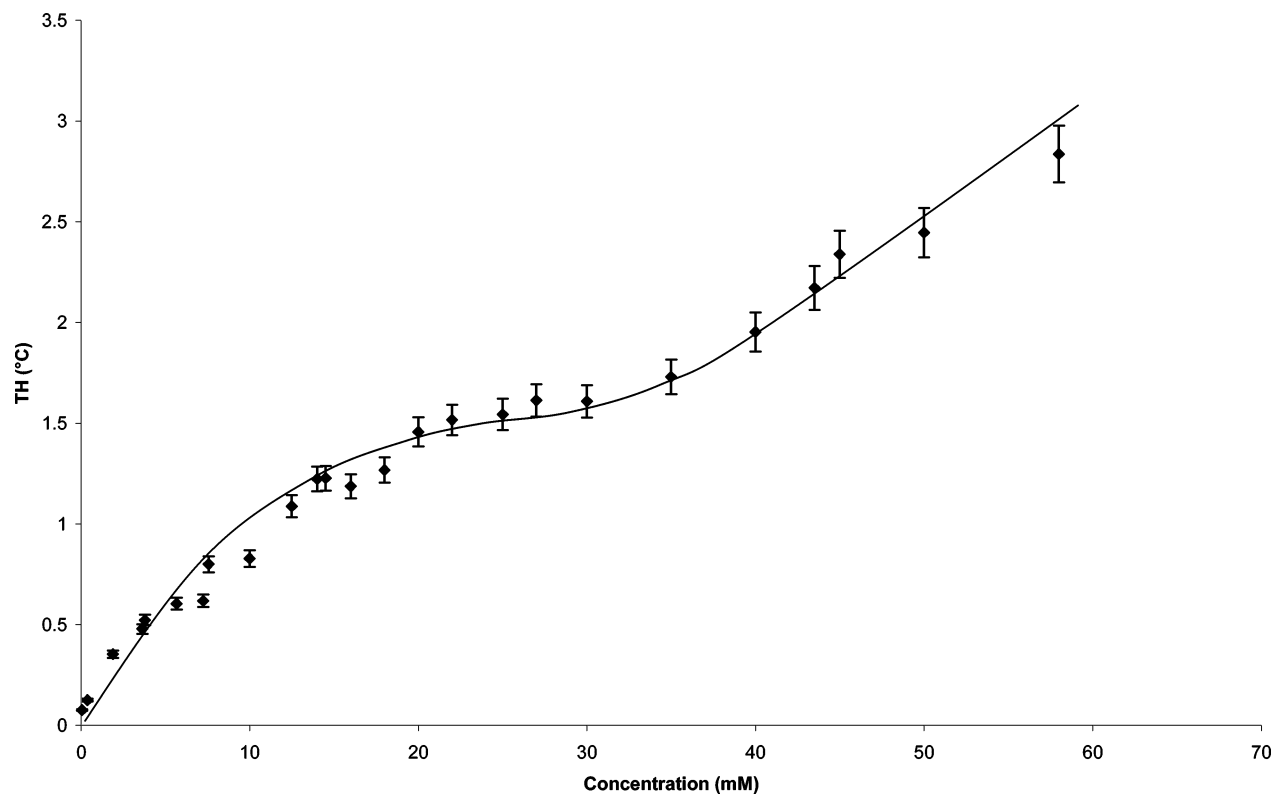


Figure 9. Thermal hysteresis activity as a function of AFGP8 concentration.

active than the dilute solutions. We believe the plateau in Figure 9 is representative of monomeric AFGP8 while the 40–60 mM solutions contain predominantly aggregated AFGP8. Interestingly, the ice crystal morphology observed with these AFGP8 solutions was indistinguishable from that of the 0.5–30 mM solutions. Given that our DLS experiments indicate a 40 mM AFGP8 solution possess a large amount of aggregates, we conclude that these aggregates are responsible for the observed increase in activity.

Discussion

Our results confirm the existence of low molecular mass aggregates in solutions of AFGP8. More specifically, we see evidence of aggregation in AFGP8 solutions that are 20 mM and greater in concentration. The size of the aggregates is different than that previously estimated by AFM experiments²³ and the formation of these aggregates is likely driven by nonionic interactions. Trends suggest that this is a complex equilibrium dependent upon concentration and time.

The solution conformation of AFGP8 at room temperature and 0 °C is largely consistent with that of random coil structure, but other secondary structures appear to be present. No obvious conformational differences resulted from temperature changes. This result is consistent with reports that AFGP8 does not undergo any global rearrangements in the supercooled regime.²⁹ Recent studies have suggested that the solution conformation of AFGP is consistent with a polyproline II structure.⁸ However, our data are consistent with a random coil structure reported from earlier CD studies.¹⁴ This apparent inconsistency may arise from the fact that the CD spectra of a random coil conformation is very similar to that of a polyproline type II³⁰ and that these two solution structures cannot be easily distinguished from each other.³¹ Alternatively, the fact that a well-defined isodichroic point was not observed in our experiments indicates that other

conformations are in equilibrium with the random coil structure, suggesting that the AFGP8 glycopeptide is highly flexible and assumes a number of solution conformations at different times (or in different molecules). This conclusion is supported by previous conformational studies of AFGP analogues.⁹

Recent NMR data suggests AFGP8 possesses significant local order over the short 14 amino acid sequence of an individual molecule but no long-range order in solution.²² This is consistent with our analysis, as the interactions giving rise to the CD signals occur over relatively short distances (10–20 Å or 5–10 amino acid residues) and it would be expected that a number of different molecules may exhibit different conformational characteristics over a short period of time due to the inherent flexibility of the glycoprotein. The net result of this intermittent ordering would be an apparent mixture of solution conformations with random coil being the predominant secondary structure.¹⁵ Given that it would be quite difficult to assume more than one secondary structure over a relatively short peptide sequence of 14 residues, it is likely that individual AFGP8 molecules are adopting different secondary structures at different times. It is also possible that the different secondary structures arise from transient or stable interactions between monomers as is often found in coiled-coil proteins. Our findings are also in agreement with conformational studies performed using Raman spectroscopy¹⁷ where the presence of a α -helix and β -sheet was observed but the major conformation was considered to be random coil.

Another interesting feature in the CD analysis of AFGP8 is the prevalence of a shift for λ_{max} to decreased wavelength (red shift) in all sample concentrations between 20 and 100 mM. This trend was observed at room temperature and 0 °C (Figures 6 and 8). While the interpretation of a red shift is controversial, it is consistent with the formation of aggregates in solution³² and consequently correlates well with the results from our DLS experiments. It appears that AFGP8 aggregation does not facilitate significant changes in solution conformation, as the

20–100 mM AFGP solutions all possess random coil structure as the predominant conformation. However, the incremental conformational changes that are observed in these more concentrated solutions (i.e., slight increases in α -helix, etc.) may be a direct result of the aggregation. These incremental changes were completely reversible and the fact that a well-defined isodichroic point did not exist suggested that more than two conformations are present in solution.

A plausible explanation for the increase in TH activity may be attributed to AFGP8 binding the ice surface as an aggregate and not a single AFGP8 molecule. The increased size of the AFGP8 aggregate (relative to a single AFGP8 molecule) would result in a decreased surface area of the exposed ice front between adjacent aggregates. As a consequence, the surface curvature in areas between adjacent aggregates would increase and the amount of energy required to incorporate additional water molecules into the ice lattice would also increase dramatically.⁴ A similar effect has been reported with AFP fusion proteins.³³ Our results are consistent with the fact that lower molecular weight fractions of AFGPs have been shown to work in a cooperative manner with larger fractions (AFGP1–5), resulting in a 2–8-fold potentiation of thermal hysteresis activity.^{34,35} However, this is the first example where lower molecular weight AFGP fractions have demonstrated such a cooperative effect in the absence of higher molecular weight fractions or other proteins. The biological significance of the increased TH activity as a function of aggregation is not understood at this time as aggregation starts to appear in solution at concentrations equal to 60 mg/mL *in vitro*. To date, such high concentrations of AFGP have not been reported *in vivo*. However, it should be noted that the smaller fractions of AFGP such as AFGP8 are typically found in much higher concentrations than the larger fractions in fish blood.

Conclusions

We have demonstrated that AFGP8 forms aggregates in solution consisting of at least two individual AFGP8 molecules. These aggregates increase in size as a function of time. The formation of aggregates appears to occur at solution concentrations greater than 20 mM. While these results confirm the propensity of AFGP8 to form aggregates in solution, the size of the aggregates observed by DLS are much smaller than was previously observed by atomic force microscopy. This may be explained by the fact that AFM resolution in the x and y dimensions is an order of magnitude better than resolution in the z dimension. Consequently, the size of the aggregates as determined by AFM would have been overestimated.

Our analyses of AFGP secondary structure in aqueous solution by CD spectroscopy suggest that random coil is the major conformation at room temperature in 0.01–100 mM solutions. However, large amounts of β -sheet and α -helix character are also present in the more concentrated solutions (i.e., 10–100 mM). A distinct red shift at concentrations between 20 and 100 mM is consistent with aggregate formation. Analysis of the same solutions at -0.5 °C revealed no significant differences in solution conformation relative to those analyzed at room temperature. The largest amount of random coil structure was seen at concentrations between 0.01 and 5 mM irrespective of temperature.

In contrast to AFGP1–5, the propensity for AFGP8 to aggregate has not been reported. This ability may be unique to the lower molecular weight AFGPs. A correlation of AFGP8 concentration and thermal hysteresis activity indicates that

aggregated AFGP8 solutions are significantly more active than the monomeric species. While the cooperative functioning of AFGPs has been demonstrated in a solution containing both AFGP8 and AFGP1–5, this is the first example in which AFGP8 demonstrates a cooperative effect in the absence of higher molecular weight fractions. The physiological implications of this are not clear as AFGP8 aggregation appears to occur at concentrations much higher than those reported in deep sea teleost fish. The interactions of the dimeric species with the ice lattice have not been addressed and will be the topic of future work.

Experimental Methods

DLS spectra were obtained on a MSX DynaPro dynamic light scattering instrument interfaced and controlled by a Dell computer. All measurements were obtained 825.2 nm and each concentration was measured 20 times with 11 acquisitions of 10 s. The viscosity of the solutions at 20 °C was presumed to be equal to 1. All the DLS experiments were performed in doubly distilled H₂O at pH 7.4. Our filtered solutions were filtered with cellulose centrifugal filters possessing a 100 kDa cutoff. As the solutions analyzed contain complex mixtures of aggregates, the traditional z -average algorithm would result in highly inconsistent data and no multimodality would be observed. Therefore in these experiments, the Dynamics software version 6.1.08 has been utilized. This software and its algorithms are consistent with the CONTIN algorithm³⁶ and consequently permit interpretation of correlation curves exhibiting multiple exponential decays.³⁷ The results of this analysis provide the diffusion coefficient (D_i) for each aggregate. The Stokes–Einstein relationship $R_{h,i} = k_B T / (6\pi\eta D_i)$ where k_B is the Boltzmann constant and η is the solvent viscosity afforded the hydrodynamic radius ($R_{h,i}$) of each aggregate. The measured hydrodynamic radius has been converted to molecular mass by use of the conventional Coil model $M_i = R_{h,i}^2 N_A 4\pi / (3V_p)$, where N_A represents Avogadro's number and V_p is the partial specific volume. A family of globular proteins has been used to estimate the relationship between the partial specific volume and aggregate size {i.e., M_i (kilodaltons) = $[(R_h \text{ factor})R_h \text{ (nanometers)}]^x$ (where $R_h \text{ factor} = 1.6800$ and $x = 2.3398$)}.³⁸

CD spectra were obtained on a Jasco Model J-810 automatic recorder spectropolarimeter interfaced with a Dell computer. All measurements were performed at 21 or -0.5 °C in quartz cells of 0.1 and 0.5 cm path length. Spectra were obtained with a 1.0 nm bandwidth time constant of 2 s and a scan speed of 50 nm/min. Eight scans were added to improve the signal-to-noise ratio, and baseline corrections were made against each sample. All the spectra were recorded between 190 and 300 nm, and all the CD experiments were performed in doubly distilled H₂O at pH 7.4. Secondary structures of the CD spectra were estimated by use of CDPro, a web-based software package available at <http://lamar.colostate.edu/~sreeram/CDPro/main.html>. The data from each spectrum were analyzed by three different deconvolution programs (SELCON3, CDSSTR, CONTINLL). Of the three programs, SELCON3 and CONTINLL gave the most consistent results. IBASIS5 was used as the set of reference proteins containing 37 proteins with α -helix, β -structure, polyproline II, and unordered conformations with optimal wavelength 185–240 nm.

AFGP8 was generously donated by A/F Protein Inc. as a lyophilized powder after extraction and purification from the Greenland cod (*Gadus ogac*).

Acknowledgment. We acknowledge the National Institutes of Health (NIH, RO1 60319), the Natural Sciences and Engineering Research Council of Canada, and the Canada Research Chair Program for financial support. In addition, Professors Natalie Goto and John Baenziger are acknowledged for their helpful suggestions. We thank Dr. Mary Hefford of Health Canada for access to the CD instrument and helpful

suggestions using the deconvolution programs. R.N.B. holds a Canada Research Chair in Medicinal Chemistry.

References and Notes

- (1) Davies, P. L.; Sykes, B. D. *Curr. Opin. Struct. Biol.* **1997**, *7*, 828–834.
- (2) Fletcher, G. L.; Hew, C. L.; Davies, P. L. *Annu. Rev. Physiol.* **1999**, *63*, 359–390.
- (3) Morris, H. R.; Thompson, M. R.; Osuga, D. T.; Ahmed, A. I.; Chan, S. M.; Vandenheede, J. R.; Feeney, R. E. *J. Biol. Chem.* **1978**, *253*, 5155–5162.
- (4) Wilson, P. W. *Cryo-Lett.* **1993**, *14*, 31–36.
- (5) Knight, C. A. *Nature* **2000**, *406*, 249–251.
- (6) Harding, M. M.; Anderberg, P. I.; Haymet, A. D. J. *Eur. J. Biochem.* **2003**, *270*, 1381–1392.
- (7) Knight, C. A.; Driggers, E.; DeVries, A. L. *Biophys. J.* **1993**, *64*, 252–259.
- (8) Tachibana, Y.; Fletcher, G. L.; Fujitani, N.; Tsuda, S.; Monde, K.; Nishimura, S. I. *Angew. Chem., Int. Ed.* **2004**, *43*, 856–862.
- (9) Filira, F.; Scolaro, B. B.; Foffani, M. T.; Mammi, S.; Peggion, R.; Rocchi, R. *Int. J. Biol. Macromol.* **1990**, *12*, 41–49.
- (10) Franks, F.; Morris, E. R. *Biochim. Biophys. Acta* **1978**, *540*, 346–356.
- (11) Rao, B. N.; Bush, C. A. *Biopolymers* **1987**, *26*, 1227–1244.
- (12) Tachibana, Y.; Matsubara, N.; Nakajima, F.; Tsuda, T.; Tsude, S.; Monde, K.; Nishimura, S.-I. *Tetrahedron* **2002**, *58*, 10213–10224.
- (13) DeVries, A. L.; Komatsu, S. K.; Feeney, R. E. *J. Biol. Chem.* **1970**, *245*, 2901–2908.
- (14) Raymond, J. A.; Radding, W.; DeVries, A. L. *Biopolymers* **1977**, *16*, 2575–2578.
- (15) Bush, C. A.; Feeney, R. E.; Osuga, D. T.; Ralapati, S.; Yeh, Y. *Int. J. Pept. Protein Res.* **1981**, *17*, 125–129.
- (16) Ahmed, A. I.; Feeney, R. E.; Osuga, D. T.; Yeh, Y. *J. Biol. Chem.* **1975**, *250*, 3344–3347.
- (17) Yomimatsu, Y.; Scherer, J. R.; Yin, Y.; Feeney, R. E. *J. Biol. Chem.* **1976**, *251*, 2290–2298.
- (18) Bush, C. A.; Feeney, R. E. *Int. J. Pept. Protein Res.* **1986**, *28*, 386–397.
- (19) Berman, E.; Allerhand, A.; DeVries, A. L. *J. Biol. Chem.* **1980**, *255*, 4407–4410.
- (20) Bush, C. A.; Ralapati, S.; Matson, G. M.; Yamasaki, R. B.; Osuga, D. T.; Yeh, Y.; Feeney, R. E. *Arch. Biochem. Biophys.* **1984**, *232*, 624–631.
- (21) Lane, A. N.; Hays, L. M.; Feeney, R. E.; Crowe, L. M.; Crowe, J. H. *Protein Sci.* **1998**, *7*, 1555–1563.
- (22) Lane, A. N.; Hays, L. M.; Tsvetkova, N.; Feeney, R. E.; Crowe, L. M.; Crowe, J. H. *Biophys. J.* **2000**, *78*, 3195–3207.
- (23) Sarno, D.; Murphy, A. V.; DiVirgilio, E. S.; Jones, W. E., Jr.; Ben, R. N. *Langmuir* **2003**, *19*, 4740–4744.
- (24) Wu, Y.; Banoub, J.; Goddard, S. V.; Kao, M. H.; Fletcher, G. L. *Comp. Biochem. Physiol., B* **2001**, *128*, 265–273.
- (25) A similar result was observed when AFGP4 polydispersity was studied by quasi-elastic light scattering (QELS or DLS). Other AFGP fractions failed to show the same polydispersity. See ref 16.
- (26) (a) Greenfield, N. J. *Anal. Biochem.* **1996**, *35*, 1–10. (b) Sreerama, N.; Venyaminov, S. Y.; Woody, R. W. *Anal. Biochem.* **2000**, *287*, 243–251. (c) Sreerama, N.; Woody, R. W. *Anal. Biochem.* **2000**, *287*, 252–260.
- (27) Woody, R. W. *J. Polym. Sci. Macromol. Rev.* **1977**, *12*, 181–320.
- (28) Greenfield, N.; Fasman, G. D. *Biochemistry* **1969**, *8*, 4108–4116.
- (29) Krishnan, V. V.; Fink, W. H.; Feeney, R. E.; Yeh, Y. *Biophys. Chem.* **2004**, *110*, 223–230.
- (30) Steim, J. M.; Fleischer, S. *Proc. Natl. Acad. Sci. U.S.A.* **1967**, *58*, 1292–1298.
- (31) Davies, P. L.; Hew, C. L. *FASEB J.* **1990**, *4*, 2460–2468.
- (32) Chakrabarty, A.; Yang, D. S. C.; Hew, C. L. *J. Biol. Chem.* **1989**, *264*, 11307–11313.
- (33) Deluca, C. I.; Comley, R.; Davies, P. L. *Biophys. J.* **1998**, *74*, 1502–1508.
- (34) Osuga, D. T.; Ward, F. C.; Yeh, Y.; Feeney, R. E. *J. Biol. Chem.* **1978**, *253*, 6669–6672.
- (35) Mulvihill, D. M.; Geoghegan, K. F.; Yeh, Y.; DeRemer, K.; Osuga, D. T.; Ward, F. C.; Feeney, R. E. *J. Biol. Chem.* **1980**, *255*, 659–662.
- (36) Provencher, S. W. *J. Chem. Phys.* **1976**, *64*, 2772;
- (37) Provencher, S. W. *Comput. Phys. Commun.* **1982**, *27*, 229–242.

BM050605T